Molecular Biology of the Cell
Vol. 21, 674–685, February 15, 2010

The Cell Surface Protein Gene *ecm33*$^+$ Is a Target of the Two Transcription Factors Atf1 and Mbx1 and Negatively Regulates Pmk1 MAPK Cell Integrity Signaling in Fission Yeast

Hirofumi Takada,* Aiko Nishida,* Mitsuhiro Domae,* Ayako Kita,* Yuki Yamano,* Atsushi Uchida,* Shunji Ishiwata,* Yue Fang,† Xin Zhou,† Takashi Masuko,‡ Mitsuhiro Kinoshita,§ Kazuaki Kakehi,§ and Reiko Sugiura*

*Laboratory of Molecular Pharmacogenomics, ‡Laboratory of Molecular and Cellular Biology, and §Laboratory of Bioinformatics, School of Pharmaceutical Sciences, Kinki University, Higashi-Osaka, 577-8502, Japan; and †Division of Molecular Pharmacology and Pharmacogenomics, Department of Biochemistry and Molecular Biology, Kobe University Graduate School of Medicine, Chuo-ku, Kobe 650-0017, Japan

Submitted September 21, 2009; Revised December 7, 2009; Accepted December 15, 2009
Monitoring Editor: Daniel J. Lew

The highly conserved fission yeast Pmk1 MAPK pathway plays a key role in cell integrity by regulating Atf1, which belongs to the ATF/cAMP-responsive element-binding (CREB) protein family. We identified and characterized *ecm33*$^+$, which encodes a glycosyl-phosphatidylinositol (GPI)-anchored cell surface protein as a transcriptional target of Pmk1 and Atf1. We demonstrated that the gene expression of Ecm33 is regulated by two transcription factors Atf1 and a MADS-box-type transcription factor Mbx1. We identified a putative ATF/CREB-binding site and an RLM1-binding site in the *ecm33*$^+$ promoter region and monitored the transcriptional activity of Atf1 or Mbx1 in living cells using a destabilized luciferase reporter gene fused to three tandem repeats of the CRE and six tandem repeats of the Rlm1-binding sequence, respectively. These reporter genes reflect the activation of the Pmk1 pathway by various stimuli, thereby enabling the real-time monitoring of the Pmk1 cell integrity pathway. Notably, the Δ*ecm33* cells displayed hyperactivation of the Pmk1 signaling together with hypersensitivity to Ca^{2+} and an abnormal morphology, which were almost abolished by simultaneous deletion of the components of the Rho2/Pck2/Pmk1 pathway. Our results suggest that Ecm33 is involved in the negative feedback regulation of Pmk1 cell integrity signaling and is linked to cellular Ca^{2+} signaling.

INTRODUCTION

The mitogen-activated protein kinase (MAPK) pathway is one of the most important intracellular signaling pathways that play a crucial role in cell proliferation, cell differentiation, and cell cycle regulation (Nishida and Gotoh, 1993; Marshall, 1994; Herskowitz, 1995; Levin and Errede, 1995). MAPKs deliver extracellular signals from activated receptors to various cellular compartments, especially, the nucleus, where they regulate eukaryotic gene expression at the transcriptional and posttranscriptional levels (Pouyssegur, 2000; Sugiura *et al.*, 2003; Edmunds and Mahadevan, 2004; Satoh *et al.*, 2009).

In the budding yeast *Saccharomyces cerevisiae*, the Slt2/Mpk1 MAPK pathway mediates cell cycle–regulated cell wall synthesis and responds to different signals, including cell cycle regulation, growth temperature, changes in external osmolarity, and mating pheromones (Gustin *et al.*, 1998). Signaling proteins involved in the pathway include the GTP-binding protein Rho1, the protein kinase C homologue Pkc1, the MEKK Bck1p/Slk1p, the redundant pair of MAP/ERK kinases (MEKs) Mkk1 and Mkk2, the MAPK Slt2/Mpk1, and the transcription factor targets Rlm1 and SBF (Gustin *et al.*, 1998). Moreover, signaling via Mpk1/Slt2-Rlm1 regulates the expression of at least 25 genes, most of which have been implicated in cell wall biogenesis (Jung and Levin, 1999; Jung *et al.*, 2002).

We have been studying the Pmk1 MAPK signaling pathway in the fission yeast *Schizosaccharomyces pombe*. The Pmk1 MAPK, a homologue of the mammalian ERK/MAPK plays a central role in cell integrity in fission yeast (Toda *et al.*, 1996; Zaitsevskaya-Carter and Cooper, 1997). The Pmk1 MAPK pathway is composed of MAPKKK Mkh1 (Sengar *et al.*, 1997), MAPKK Pek1 (Sugiura *et al.*, 1999), and MAPK Pmk1/Spm1. The Pmk1 MAPK pathway also regulates ion homeostasis and morphogenesis (Satoh *et al.*, 2009) and is activated under multiple stresses, including heat shock, hyper- or hypotonic stresses, cell wall damage, or glucose deprivation (Toda *et al.*, 1996; Sugiura *et al.*, 1999; Madrid *et al.*, 2006).

We have previously demonstrated that calcineurin and Pmk1 MAPK play antagonistic roles in Cl^- homeostasis (Sugiura *et al.*, 1998, 2002) and genetic screening on the basis of the functional interaction between calcineurin and Pmk1 MAPK has resulted in the isolation of negative regulators of the Pmk1 MAPK pathway, including *pmp1*$^+$, encoding a

This article was published online ahead of print in *MBC in Press* (http://www.molbiolcell.org/cgi/doi/10.1091/mbc.E09–09–0810) on December 23, 2009.

Address correspondence to: Reiko Sugiura (sugiurar@phar.kindai.ac.jp).

dual-specificity MAPK phosphatase (Sugiura *et al.*, 1998); *pek1*$^+$, encoding a MAPK kinase (MAPKK; Sugiura *et al.*, 1999); and *rnc1*$^+$, encoding a novel KH-type RNA-binding protein that stabilizes Pmp1 mRNA (Sugiura *et al.*, 2003, 2004). Moreover, genetic screening for *vic* (viable in the presence of immunosuppressant and chloride ion) mutants revealed that the *cpp1*$^+$ gene, encoding a β subunit of the protein farnesyltransferase, and its target Rho2 GTPase (Ma *et al.*, 2006) act as upstream regulators of the Pmk1-signaling pathway.

Most recently, we have identified the Atf1 transcription factor as a downstream target of the Pmk1 MAPK pathway and demonstrated that Atf1 is involved in cell integrity in addition to its well-established role in the stress responses mediated by the Sty1/Spc1 MAPK pathway in fission yeast (Takada *et al.*, 2007). Mbx2, an Rlm1 homologue in fission yeast, unlike in budding yeast, displayed only a modest sensitivity to cell wall–damaging agents, suggesting that Mbx2 plays a minor role in this process (Takada *et al.*, 2007). Moreover, the intermediate phenotypes of the Δ*atf1* cells in the cell integrity response suggest that other unidentified target(s) of Pmk1 must play a significant role in the cell integrity pathway in fission yeast.

To identify novel genes involved in cell integrity signaling pathway, we searched for *S. pombe* homologues of the cell wall biogenesis genes regulated by the Mpk1-Rlm1 pathway in budding yeast. Of these genes, PST1 was particularly interesting because its gene expression was induced upon exposure to various cell wall–damaging agents such as azole and polyene under the control of the Slt2/Rlm1 signaling (Jung and Levin, 1999; Agarwal *et al.*, 2003). Hence, we speculated that the fission yeast homologue of PST1 might serve as a good candidate for the target of Pmk1 signaling, as well as a good tool for studying the activation mechanism of Pmk1.

In the present study, we focused on *ecm33*$^+$ (SPAC1705.03c) that encodes a glycosyl-phosphatidylinositol (GPI)-anchored cell surface protein, which is similar to ECM33 and PST1 in budding yeast, and characterized the expression mechanism and the role of Ecm33 in the Pmk1-mediated cell integrity signaling. Notably, Ecm33 expression was found to be regulated by two transcription factors, namely, Atf1 and Mbx1, via the putative cAMP-responsive element (CRE) sequence TTACAGTAA and the RLM1-binding sequence GTATATATAG in the promoter region of the *ecm33*$^+$ gene. Furthermore, we developed reporter systems that allowed the monitoring of the real-time activity of Atf1 and Mbx1 in living cells by constructing a destabilized luciferase reporter gene with a reduced functional half-life fused to three tandem repeats of the CRE ($3x\text{CRE}_{\text{ecm33}}$::luc) or six tandem repeats of the Rlm1-binding sequence ($6x\text{Rlm1}_{\text{ecm33}}$::luc). These reporter constructs also reflected the Pmk1 activity, thereby enabling the monitoring of the activation of the cell integrity pathway. We also presented evidence that Ecm33 is involved in the Pmk1 signaling by affecting Ca^{2+} homeostasis in fission yeast.

MATERIALS AND METHODS

Strains, Media, and Genetic and Molecular Biology Methods

S. pombe strains used in this study are listed in Table 1. The complete medium YPD (yeast extract-peptone-dextrose) and the minimal medium EMM (Edinburgh minimal medium) have been described previously (Toda *et al.*, 1996). Standard genetic and recombinant DNA methods (Moreno *et al.*, 1991) were used, except where specified. FK506 was provided by Astellas Pharma (Osaka, Japan). An *S. pombe* haploid strain in which the *sty1*$^+$/*spc1*$^+$ gene (geneID SPAC24B11.06c) had been deleted was purchased from Bioneer (Daejeon, Korea).

Table 1. *Schizosaccharomyces pombe* strains used in this study

Strain	Genotype	Reference
HM123	*h*$^-$ *leu1-32*	Our stock
KP456	*h*$^-$ *leu1-32 ura4-D18*	Our stock
KP208	*h*$^-$ *leu1-32 ura4-D18 pmk1::ura4*$^+$	Our stock
KP119	*h*$^+$ *leu1-32 ura4-D18 ppb1::ura4*$^+$	Our stock
KP2163	*h*$^-$ *leu1-32 pck2::KanMx6*	Our stock
KP471	*h*$^-$ *leu1-32 ura4-D18 spc1::ura4*$^+$	Our stock
KP495	*h*$^-$ *leu1-32 ura4-D18 atf1::ura4*$^+$	Our stock
KP2178	*h*$^-$ *leu1-32 pmk1::KanMx6*	Satoh *et al.* (2009)
KP2118	*h*$^-$ *leu1-32 ura4-D18 pmk1::KanMx6*	Satoh *et al.* (2009)
SP655	*h*$^-$ *leu1-32 ura4-D18 ecm33::ura4*$^+$	This study
SP632	*h*$^-$ *leu1-32 ura4-D18 meu10::ura4*$^+$	This study
SP550	*h*$^-$ *leu1-32 ura4-D18 mbx1::ura4*$^+$	This study
SP587	*h*$^-$ *leu1-32 mbx2::KanMx6*	This study
SP674	*h*$^-$ *leu1-32 ura4-D18 mbx1::KanMx6*	This study
SP977	*h*$^-$ *leu1-32 ura4-D18 ecm33::ura4*$^+$ *pmk1::KanMx6*	This study
SP1220	*h*$^+$ *leu1-32 ura4-D18 ade6-M210 sty1::KanMx4*	Bioneer

Cloning and Knockout of the ecm33$^+$ Gene

The *ecm33*$^+$ gene was amplified by PCR using the genomic DNA of *S. pombe* as a template. The sense primer used for PCR was 5′-GAA GAT CTC ATG TTG TTC AAA TCA TTC GCT CTC ACT C-3′ (BglII site and start codon are underlined), and the antisense primer was 5′-GAA GAT CTG CGG CCG CCC ATA GCA AGA GCA GCA ACC AAA AGA G-3′ (BglII and NotI site are underlined). The amplified product was digested with BglII/NotI, and the resulting fragment was subcloned into Bluescript SK(+) to create pBS-ecm33.

To knockout the *ecm33*$^+$ gene, a one-step gene disruption by homologous recombination was performed (Rothstein, 1983). The *ecm33*$^+$ null mutants were obtained by entire deletion of the corresponding coding sequence and its replacement with the *ura4*$^+$ cassette by PCR-mediated strategy using plasmid pFA6a-ura4 as the template (Bahler *et al.*, 1998).

The ecm33$^+$ Promoter Assay

Firefly luciferase was chosen as a reporter, because the assay is simple to perform and has a high signal-to-noise ratio (Leskinen *et al.*, 2003). A 0.5-kb DNA fragment (P0.5, 500/2 base pairs) in the 5′ flanking region of the *ecm33*$^+$ gene was amplified by PCR primers (forward primer 170, 5′-AA CTG CAG CAA GCT CCT CGT TGG TGT TGT GGCC-3′; reverse primer 126, 5′-CCG CTC GAG ATT GAC TTT AGA CTA TAT AAT GTA GAA ATA TG-3′). Similarly, the 5′-end deletion mutants of P0.5 (P0.45, 450/2 base pairs; P0.4, 402/2 base pairs; P0.37, 369/2 base pairs; and P0.3, 300/2 base pairs) were prepared using the reverse primer 126 and the following forward primers: 228 (5′-AA CTG CAG CAT TGT TTA CAG TAA ACA TTG CAA CG-3′), 229 (5′-AA CTG CAG CCT TTT TAT CTA ACA AGT CAC AAT TC-3′), 192 (5′-AA CTG CAG TTT CCG GGT ATA TAT AGA TGT CTT TTC CGC-3′), and 171 (5′-AA CTG CAG ACA CTC TTT TAC TTC TTT ATT CAT TAC CC-3′). The 3′-end deletion mutants of P0.5 (P0.2, 200/2 base pairs; and P0.1, 100/2 base pairs) were prepared using the forward primer 170 and the following reverse primers: 230 (5′-CCG CTC GAG TTA AAA CTC AAA TGT AGT TCG CTG-3′) and 257 (5′-CCG CTC GAG AAG GGG GAC AAC GAG GTG CGC-3′). The 5′-end and 3′-end deletion mutant of P0.5 (P0.07, 69/2 base pairs) was prepared using the forward primer 192 and the reverse primer 230. The various fragments of the 5′ promoter region of *ecm33*$^+$ were subcloned into the PstI/XhoI-digested pKB5723 (Deng *et al.*, 2006), a multicopy vector that contains the destabilized luciferase gene from pGL3 (R2.2; Promega, Madison, WI).

Cells transformed with these reporter plasmids were cultured at 27°C in EMM to midlog phase. The *ecm33*$^+$ promoter activity was measured as described by Deng *et al.* (2006), with minor modifications. Briefly, the culture was diluted with fresh medium to $OD_{660} = 0.2$, and the cells were grown for 3 h at 27°C. Cells were incubated with 0.5 mM D-luciferin for 10 min at 27°C. Aliquots of the cell culture were pipetted into a 96-well plate, and NaCl was added to a final volume and concentration of 100 μl and 500 mM, respectively. Distilled water, which was used as control, was added to some of the wells. The mixture was incubated at 27°C for 2 h, and light emission levels expressed as relative light units were measured using a luminometer (AB-2300; Atto, Tokyo, Japan) at 12-s intervals.

Live-Cell Monitoring of Pmk1-mediated Transcriptional Activity

A 1.2-kb PstI/XhoI fragment of pKB5721 was replaced with the *ecm33*$^+$-derived CRE oligonucleotide (sense 259: 5′-GGC TTT TAC AGT AAA TAC ATT ACA GTA AAT ACA CAT TAC AGT AAA TGC AC-3′, antisense 260:

5′-TCG AGT GCA TTT ACT GTA ATG TGT ATT TAC TGT AAT GTA TTT ACT GTA AAA GCC TGCA-3′) that contains three tandem repeats of CRE (TTACAGTAA or TTACTGTAA, underlined), which is the Atf1-binding core identified in the *ecm33*$^+$ promoter, to yield pKD1934.

The point-mutated CRE reporter (pKD1953) was obtained in the same way as the CRE mutant (Pascual-Ahuir *et al.*, 2001) oligonucleotide (sense 269: 5′-GGC TTT TAT TTT AAA TAC ATT ATT TTA AAT ACA CAT TAT TTT AAA TGC AC-3′, antisense 270: 5′-TCG AGT GCA TTT AAA ATA ATG TGT ATT TAA AAT AAT GTA TTT AAA ATA AAA GCC TGCA-3′) that contains the three tandem repeats of the CRE mutant (TTATTTTAA or TTAAAATAA, underlined). Similarly, a 1.2-kb PstI/XhoI fragment of pKB5721 was replaced with the *ecm33*$^+$-derived RLM1 oligonucleotide (sense 341: 5′-GGC TTG TAT ATA TAG ATA CAG TAT ATA TAG ATA CAC AGT ATA TAT AGA TAC AGT ATA TAT AGA TAC ACA GTA TAT ATA GAT ACA GTA TAT ATA GAT GCAC-3′, antisense 342: 5′-TCG AGT GCA TCT ATA TAT ACT GTA TCT ATA TAT ACT GTG TAT CTA TAT ATA CTG TAT CTA TAT ATA CTG TGT ATC TAT ATA TAC TGT ATC TAT ATA TAC AAG CCT GCA-3′) that contains six tandem repeats of RLM1 (GTATATATAG or CTATATATAC, underlined), which is the Mbx1-binding core identified in the *ecm33*$^+$ promoter, to yield pKD1936.

The point-mutated RLM1 reporter (pKD1991) was obtained in the same way as the MEF2 mutant (Thai *et al.*, 1998) oligonucleotide (sense 367: 5′-GGC TTG TGG GCC CAG ATA CAG TGG GCC CAG ATA CAC AGT GGG CCC AGA TAC AGT GGG CCC AGA TAC ACA GTG GGC CCA GAT ACA GTG GGC CCA GAT GCA C-3′, antisense 368: 5′-TCG AGT GCA TCT GGG CCC ACT GTA TCT GGG CCC ACT GTG TAT CTG GGC CCA CTG TAT CTG GGC CCA CTG TGT ATC TGG GCC CAC TGT ATC TGG GCC CAC AAG CCT GCA-3′) that contains six tandem repeats of the RLM1 mutant (GTGGGCCCAG or CTGGGCCCAC, underlined).

These reporter vectors were used for live-cell monitoring of Pmk1-mediated transcriptional activity in living cells.

Northern Blot Analyses

Total RNA was isolated by the method of Kohrer and Domdey (1991). A 20-μg sample of total RNA/lane was subjected to electrophoresis on denaturing formaldehyde 1% agarose gels and transferred to nylon membranes. Hybridization was performed using digoxigenin (DIG)-labeled antisense cRNA probes coding for Ecm33 and Leu1 as previously described (Hirayama *et al.*, 2003). The DIG-labeled hybrids were detected by an enzyme-linked immunoassay (ELISA) using an anti-DIG alkaline phosphatase antibody conjugate. The hybrids were visualized by chemiluminescence detection on a light-sensitive film according to the manufacturer's instructions (Roche Applied Science, Indianapolis, IN).

Miscellaneous Methods

Cell extract preparation and immunoblot analysis were performed as previously described (Sio *et al.*, 2005).

Ecm33 Monoclonal Antibody

Monoclonal antibody against Ecm33 was raised by using purified Ecm33 from *S. pombe*. For the first immunization, F344/N rats were subcutaneously injected with Ecm33 (50 μg protein in each rat) dissolved in 500 μl of saline emulsified with an equal volume of complete Freund's adjuvant (Difco, Detroit, MI) at multiple sites. After 3 wk, the rats were subcutaneously and intraperitoneally injected with Ecm33 (total 50 μg protein in each rat) dissolved in 500 μl of saline emulsified with an equal volume of incomplete Freund's adjuvant (Difco). A rat, the serum of which showed strong reactivity with purified Ecm33 expressed in *S. pombe* and *E. coli*, received final intraperitoneal and intravenous injections of Ecm33 (total 50 μg protein) without adjuvant. After 3 d, the rat was killed, and spleen cells were fused with P3X63Ag8.653 mouse myeloma cells, as described previously (Ohno *et al.*, 2008). Antibody secreted from 1920 hybridoma cultures was screened for reactivity with purified Ecm33 and unrelated proteins using ELISA and immune blotting. One selected hybridoma was cloned twice by the limiting dilution method. A monoclonal antibody designated 2P11 (rat IgG, κ) secreted by cloned hybridoma cells was used as a culture supernatant or as a purified monoclonal antibody as follows. Cloned hybridoma cells were intraperitoneally injected into KSN nude mice (3.0×10^6 cells/mouse) pretreated with 2,6,10,14-tetramethylpentadecane (500 μl/mouse; Pristane; Wako, Osaka, Japan). IgG in the ascites fluid was purified on protein G Sepharose (BD Healthcare, Uppsala, Sweden).

Immunostaining of Whole Cells

Cells were treated with PEMS (100 mM PIPES, pH 6.9, 1 mM EGTA, 1 mM $MgSO_4$, 1 M sorbitol) containing zymolyase 20T (0.3 mg/ml) at 37°C until ~10% of the cells lost their cell walls, as observed under a microscope. Subsequently, the cells were washed with PBS three times and were incubated for 2 h at 4°C with 100 μl of 1% BSA-PBS containing anti-Ecm33 monoclonal antibodies (20 μg/ml). After incubation, the cells were washed three times with PBS and treated with 1:300-diluted FITC-conjugated goat anti-rat immunoglobulin (Sigma, St. Louis, MO) in 100 μl of 1% BSA-PBS in the dark for 1 h at 4°C.

Measurement of Cytosolic Free Ca^{2+} Concentration Using Aequorin

The intracellular free Ca^{2+} concentration was determined using a previously described method with minor modifications (Deng *et al.*, 2006). In brief, cells containing pREP1-AEQ (apoaequorin) were grown in EMM medium and harvested in the early logarithmic growth phase. Cells were resuspended in fresh EMM containing 10 μM coelenterazine, and the optical density of a 1-ml sample was adjusted to 0.6 at 660 nm. To convert the AEQ to aequorin, the cells were incubated for 4 h at 27°C. The cells were washed three times by centrifugation and resuspension in fresh EMM. The cells were then resuspended in EMM with an optical density of 0.6 at 660 nm for a 1-ml sample, and the cell culture was incubated at 27°C for 30 min before starting the experiment. The light emission levels expressed as relative light units were measured using the luminometer at 12-s intervals.

RESULTS

Identification of the ecm33$^+$ Gene as a Target of Pmk1 and Atf1

To identify novel genes involved in the Pmk1 cell integrity signaling pathway, we searched for *S. pombe* homologues of the cell wall biogenesis genes regulated by the Mpk1-Rlm1 pathway in budding yeast (Jung and Levin, 1999). Here, we focus on the *ecm33*$^+$ gene (SPAC1705.03c) encoding a putative GPI-anchored cell surface protein (De Groot *et al.*, 2003), which is similar to PST1 (30% identity) and ECM33 (28% identity) in budding yeast (Pardo *et al.*, 2004).

Northern blot analysis demonstrated that under unstressed conditions, the *ecm33*$^+$ (SPAC1705.03c) mRNA level was significantly reduced in Δ*atf1* cells and Δ*pmk1* cells compared with that in wild-type cells (Figure 1A), suggesting that the expression of *ecm33*$^+$ is regulated by Pmk1/Atf1 signaling. Here, we characterized the *ecm33*$^+$ gene as a transcriptional target of Pmk1 and Atf1. The Δ*ecm33* cells, like Δ*pmk1* cells and Δ*atf1* cells, were highly sensitive to calcofluor, a cell wall–damaging agent (Figure 1B, +1.4 μg/ml calcofluor). Notably, the sensitivity of Δ*ecm33* cells to calcofluor was higher than that of Δ*pmk1* cells and Δ*atf1* cells to this agent (Figure 1B, +1.2 μg/ml calcofluor). The cell integrity defect associated with the Δ*ecm33* cells was further confirmed using β-glucanase, another cell wall–damaging agent. As shown in Figure 1C, the Δ*ecm33* cells showed hypersensitivity to β-glucanase as did Δ*pmk1* cells. The Δ*atf1* cells showed intermediate response to β-glucanase compared with the responses of the wild-type cells and Δ*pmk1* cells (Figure 1C). Disruption of the *meu10*$^+$ gene (Tougan *et al.*, 2002), which also shows significant amino acid similarity to PST1 and ECM33, did not result in cell wall defects (Figure 2E); therefore, we focused on the *ecm33*$^+$ gene.

To examine the expression and regulation of the *ecm33*$^+$ gene in more detail, we developed a reporter construct containing a 0.5-kb sequence upstream of ATG of the *ecm33*$^+$ gene fused to the destabilized version of luciferase R2.2 [ecm33 P(0.5)(R2.2)]. As shown in Figure 1D, the *ecm33*$^+$ promoter analysis using [ecm33 P(0.5)(R2.2)] yielded similar results as obtained by Northern blot analysis under unstressed conditions (Figure 1D, basal). We further investigated whether the expression of the *ecm33*$^+$ reporter gene was Pmk1- and Atf1-dependent under stress conditions. For this, we examined the effects of various stimuli, which have been reported to activate Pmk1 MAPK (Madrid *et al.*, 2006), on the *ecm33*$^+$ reporter expression. As expected, NaCl (500 mM), $CaCl_2$ (400 mM), KCl (400 mM), calcofluor (2.0 μg/ml), and micafungin (4.0 μg/ml) induced the expression of the *ecm33*$^+$ reporter gene in wild-type cells (Figure 1D, wt). In contrast, this induction was almost completely abolished in Δ*pmk1* cells and Δ*atf1* cells (Figure 1D). Moreover, the overexpression of Pek1^{DD}, the constitutively active version of MAPKK for Pmk1, increased the levels of the Ecm33

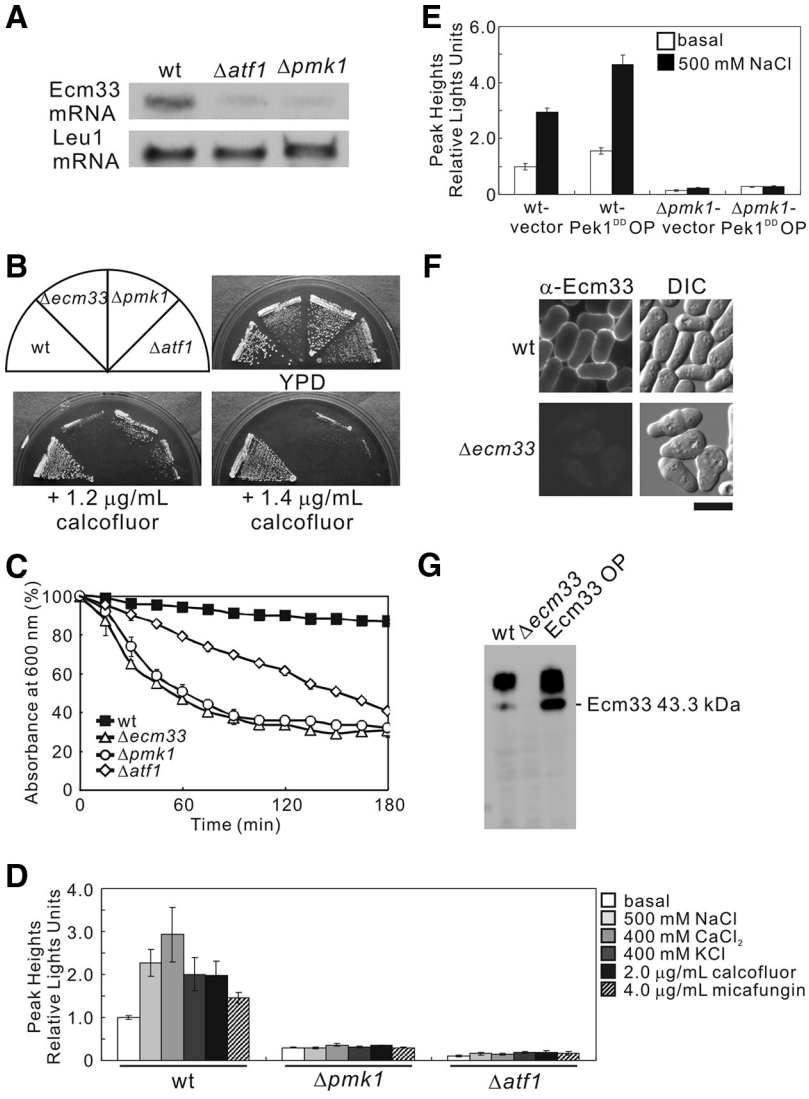

Figure 1. Identification of Ecm33 as a target of Pmk1 and Atf1. (A) Northern blot analysis of total RNA from the wild-type (wt), Δ*atf1* cells, and Δ*pmk1* cells. Cells were incubated in YPD medium and collected after culture. Total RNA (20 μg) was subjected to Northern blot analysis using a digoxigenin (DIG)-labeled Ecm33 or Leu1 cRNA. (B) The Δ*ecm33* cells showed hypersensitivity to calcofluor. Wild-type, Δ*ecm33*, Δ*pmk1*, and Δ*atf1* cells were streaked onto the plates as indicated and incubated for 4 d at 27°C. (C) The Δ*ecm33* cells showed hypersensitivity to β-glucanase. Cell lysis was measured at different times during treatment with β-glucanase by determining the OD_{600}. The strains examined were wt, Δ*ecm33*, Δ*pmk1*, and Δ*atf1*. (D) Ecm33 (P0.5R2.2) reporter expression is dependent on Pmk1-Atf1 signaling. Ecm33 expression was monitored using the luciferase reporter construct containing the 0.5-kb sequence upstream of ATG of the *ecm33*$^+$ gene [ecm33 P(0.5)(R2.2)] transformed in wild-type (wt), Δ*pmk1*, and Δ*atf1* cells. Cells were grown in YPD (basal) or subjected to various stimuli as indicated for 30 min at 27°C, and the assay was performed as described in Deng *et al.* (2006); data from at least three independent experiments are expressed as mean ± SD. (E) Overexpression of constitutively active Pek1 MAP kinase kinase stimulates Ecm33 expression. Wild-type or Δ*pmk1* cells harboring [ecm33 P(0.5)(R2.2)] were transformed with either pREP41-$Pek1^{DD}$ ($Pek1^{DD}$ OP) or the control vector (vector) and cultured for 24 h in the absence of thiamine. Cells were either untreated (basal) or treated with 500 mM NaCl. The data were averaged from peak heights of three independent experiments, and each sample was analyzed in triplicate. Error bars, SD. (F) The Ecm33 protein localizes to the cell surface. Immunofluorescence microscopy using anti-Ecm33 antibodies. Exponentially growing wild-type cells were fixed and processed for immunofluorescence microscopy using anti-Ecm33 antibodies (α-Ecm33). Scale bar, 10 μm. (G) Ecm33 monoclonal antibodies specifically recognized the Ecm33 protein. Extracts from wild-type cells containing either the multicopy plasmid carrying *ecm33*$^+$ or the control vector and Δ*ecm33* were subjected to SDS-PAGE analysis followed by immunoblot analysis with the Ecm33 antibodies.

reporter gene under unstressed conditions (Figure 1E, wt+$Pek1^{DD}$ OP, basal). Notably, the effect of overexpressing $Pek1^{DD}$ and addition of NaCl (500 mM) seemed to be additive because the reporter response was elevated (Figure 1E, wt+$Pek1^{DD}$ OP, 500 mM NaCl). Knockout of the *pmk1*$^+$ gene abolished the effects of $Pek1^{DD}$ overexpression as well as of the addition of NaCl (Figure 1E, Δ*pmk1*).

The subcellular localization of Ecm33 was determined using anti-Ecm33 antibody (α-Ecm33) by immunofluorescence microscopy. As shown in Figure 1F, Ecm33 localized to the cell surface. Immunoblotting experiments using anti-Ecm33 antibodies showed that the 43.3-kDa protein was detected in the wild-type cells (wt) and in the cells overproducing the *ecm33*$^+$ gene (Ecm33 OP), but not in Δ*ecm33* cells, indicating that the antibodies specifically recognized the Ecm33 protein (Figure 1G).

Deletion Analysis of the ecm33$^+$ *Promoter*

To determine the promoter region involved in the Pmk1-dependent ecm33 expression, the 5′ deletion mutants of the 0.5-kb DNA fragment (P0.5) of the *ecm33*$^+$ gene promoter were generated and subcloned into the multicopy luciferase vector (Figure 2A). These plasmids were transformed into a wild-type strain, and the promoter assay was performed under basal conditions (Figure 2B, basal, and Table 2). Deletion of the 5′-flanking sequences from −500 to −450 had little effect on the reporter activity (Table 2). Deletion of the region from −450 to −402 reduced the promoter activity by ~54% (Figure 2B, pKD1361). The luciferase reporter construct containing the 0.3-kb sequence upstream of ATG of the *ecm33*$^+$ gene (P0.3R2.2; Figure 2A, pKD1193) showed almost no detectable promoter activity (Figure 2B, 300–1, basal). Moreover, the luciferase reporter constructs containing the region from −500 to −300 (pKD1952, pKD1361, and pKD1360) displayed an enhanced promoter activity in response to a variety of Pmk1-activating stimuli as shown in Figure 1D, whereas the same stresses failed to induce the promoter activity of (P0.3R2.2; Figure 2B). On the basis of these results, we conclude that the region from −500 to −300 base pairs upstream of ATG of the *ecm33*$^+$ gene is important for its regulated expression.

A database search (TESS SEARCH) revealed a CRE-like sequence motif TTACAGTAA at position −444 to −436 (Figure 2, A and C, CRE, underlined) and a sequence similar to the RLM1-binding motif GTATATATAG at position −362 to −353 (Figure 2, A and C, RLM1, underlined) of the *ecm33*$^+$ gene. The presence of putative consensus elements

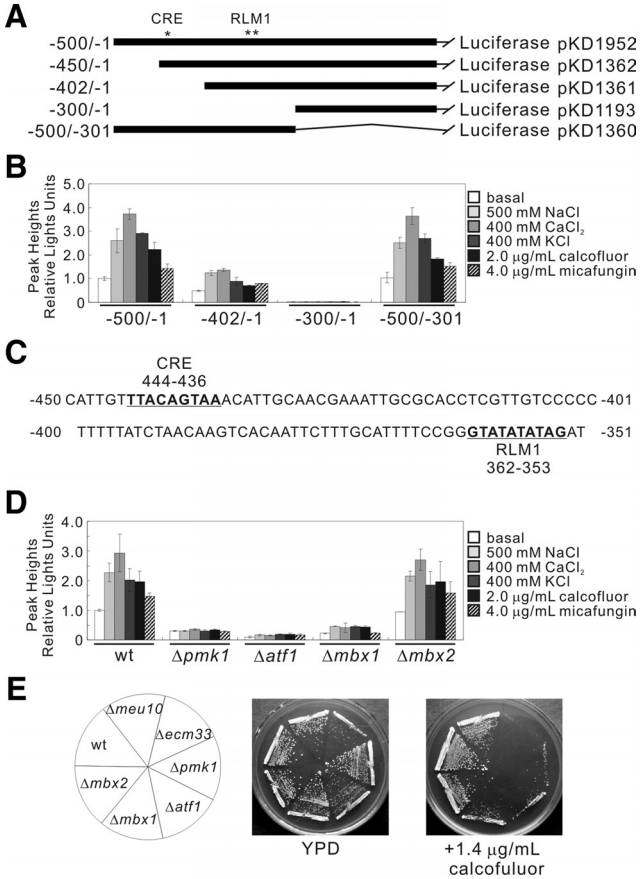

Figure 2. Promoter analysis of *ecm33*$^+$ gene. (A) Deletion analysis of the *ecm33*$^+$ promoter. Segment from the *ecm33*$^+$ upstream region indicated at the left was inserted into the multicopy plasmid containing the luciferase reporter gene. The positions of the CRE (*) and the RLM1 (**) sequences are shown. The numbers refer to the position of the deletion end point relative to the first base of the initiation codon of the gene, which are designated as +1. (B) The upstream region from −500 to −300 of the *ecm33*$^+$ gene regulates Pmk1-responsive expression of the *ecm33*$^+$ gene. The luciferase fusion plasmids as indicated were transformed into wild-type cells. Cells were either untreated (basal) or were treated with various stimuli as indicated, and the assay was performed as described in Figure 1E. (C) Identification of CRE and RLM1 in the promoter region of the *ecm33*$^+$ gene. The sequences of the CRE-like motif (TTACAGTAA) and the RLM1-like motif (GTATATATAG) identified in the *ecm33*$^+$ promoter are underlined. The numbers refer to the first and last nucleotides of the displayed sequences. (D) The Mbx1 transcription factor is involved in the Ecm33 expression. The luciferase fusion plasmid Ecm33 (P0.5R2.2) was transformed into various strains as indicated. Cells were either untreated (basal) or treated with various stimuli as indicated, and the assay was performed as described in Figure 2B. (E) The Δ*mbx1*, but not the Δ*mbx2* cells, showed hypersensitivity to calcofluor. The cells as indicated were streaked onto the plates and then incubated for 4 d at 27°C.

for the binding of the Rlm1-like transcription factor as well as the ATF1/cAMP-responsive element-binding (CREB) family protein in the promoter region of the *ecm33*$^+$ gene from −500 to −300 upstream of ATG prompted us to examine the involvement of Mbx1-like transcription factors in the regulation of Ecm33 expression. Next, we examined the promoter activity of p0.5(R2.2) in deletion mutant cells of Mbx1-like transcription factor genes, namely, Δ*mbx1* and Δ*mbx2*, and compared them with the promoter activities of the Δ*atf1*, Δ*pmk1*, or wild-type cells. Notably, disruption of

Table 2. Promoter analysis of the *ecm33*$^+$ gene

Promoter	No NaCl	+500 mM NaCl	Fold activation
−500/−1	1.00 ± 0.07	2.60 ± 0.20	2.6
−450/−1	0.90 ± 0.16	2.16 ± 0.15	2.4
−402/−1	0.49 ± 0.07	1.24 ± 0.09	2.5
−300/−1	0.01 ± 0.01	0.01 ± 0.11	0.9
−500/−301	1.04 ± 0.21	2.52 ± 0.09	2.4

A 0.5-kb DNA fragment (P (2.2)) of the *ecm33*$^+$ gene promoter, its 5′-end deletion mutants and 3′-end deletion mutants were subcloned into the multicopy plasmid containing the wild-type luciferase reporter gene and the assay was performed as described in *Materials and Methods*. Values from at least three independent experiments are expressed as mean ± SD.

the *mbx1*$^+$ gene, but not the Rlm1-homologous gene *mbx2*$^+$, resulted in a significant reduction of the Ecm33 promoter activity compared with that of the wild-type cells (Figure 2D). The relative promoter activity of the Δ*mbx1* cells was almost equivalent to that of the Δ*pmk1* cells, but was slightly higher than that of the Δ*atf1* cells (Figure 2D). Moreover, deletion of Mbx1, but not Mbx2, abrogated the induction of promoter response by various stimuli, which activate the Pmk1 pathway (Figure 2D). Similarly, disruption of the *mbx1*$^+$ gene, but not the *mbx2*$^+$ gene, resulted in the hypersensitivity to calcofluor (1.4 μg/ml) as observed in Δ*pmk1*, Δ*atf1*, or Δ*ecn33* cells (Figure 2E). Thus, we concluded that the Mbx1 transcription factor is also involved in the cell integrity pathway by regulating Ecm33 expression.

Real-Time Monitoring of Atf1 Activity in Living Cells

Atf1 activity in living cells was monitored by 3*x*CRE$_{ECM33}$ fused to R2.2 destabilized luciferase [3*x*CRE$_{ECM33}$::luc (R2.2)]. As shown in Figure 3A, wild-type cells harboring the multicopy 3*x*CRE$_{ECM33}$::luc (R2.2) reporter were stimulated by the addition of 500 mM NaCl, a hyperosmotic stress that is reported to stimulate Atf1 activity (Wilkinson *et al.*, 1996). Elevated extracellular NaCl caused an extremely rapid increase in the 3*x*CRE$_{ECM33}$::luc (R2.2) reporter response within 3 min, followed by a rapid decrease to reach its lowest value at around 30 min, then again showed a second increase, and finally approached a constant level (Figure 3A, wt). In contrast, the Δ*atf1* cells harboring the same reporter showed minimal responses to the same stimuli, indicating that multicopy 3*x*CRE$_{ECM33}$::luc (R2.2) reporter appears to be a reliable reporter of Atf1 activity (Figure 3A, Δ*atf1*). To examine whether this CRE site was of functional relevance, we used PCR primers to mutate the −444/−436 element. Compared with the wild-type promoter 3*x*CRE$_{ECM33}$::luc (R2.2) reporter, mutation in the CRE element caused a marked reduction of the promoter activity with (500 mM NaCl) or without (0 mM NaCl) the stimuli [Figure 3A, 3*x*CREm$_{ECM33}$::luc (R2.2)].

We also examined whether the 3*x*CRE$_{ECM33}$::luc (R2.2) reporter expression was dependent on two upstream MAPK pathways that phosphorylate and regulate Atf1, namely, the Sty1/Spc1 MAPK and the Pmk1 MAPK pathways. As shown in Figure 3B, the reporter expression of the 3*x*CRE$_{ECM33}$::luc (R2.2) in Δ*sty1* cells was barely detectable both in the absence and presence of a hyperosmotic stress. In addition, the 3*x*CRE$_{ECM33}$::luc (R2.2) promoter activity was very low in Δ*pmk1* cells compared with that in the wild-type cells and responded only weakly to the hyperosmotic stress

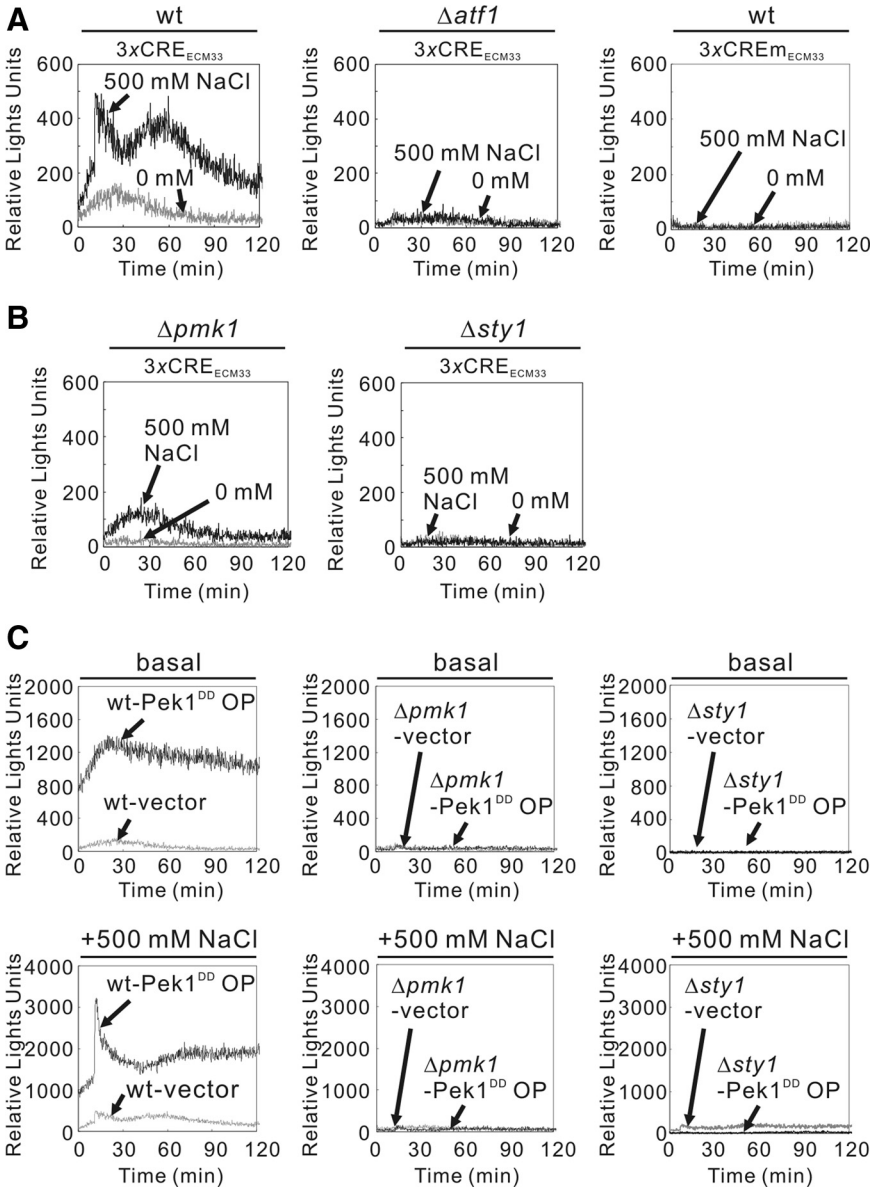

Figure 3. Real-time monitoring of Atf1 activity in living cells. (A) Wild-type cells or Δ*atf1* cells harboring the multicopy plasmid [3*x*CRE$_{ECM33}$::luc(R2.2) reporter vector] or the mutant version of the reporter vector [3*x*CREm$_{ECM33}$::luc(R2.2)] were incubated with D-luciferin and treated with 500 mM NaCl. Using a luminometer, light emission levels expressed as relative light units were measured per minute for 2 h. The data shown are representative of multiple experiments. (B) Live-cell monitoring of Atf1 activity in Δ*pmk1* cells and Δ*sty1* cells. The cells as indicated were transformed with the multicopy plasmid [3*x*CRE$_{ECM33}$::luc(R2.2) reporter vector] and analyzed as described in A. (C) Overexpression of constitutively active Pek1 MAP kinase kinase stimulates Atf1 activity. Wild-type, Δ*pmk1,* or Δ*sty1* cells harboring the multicopy plasmid [3*x*CRE$_{ECM33}$::luc(R2.2) reporter vector] were transformed with either pREP2-Pek1^{DD} (Pek1^{DD} OP) or the control vector (vector) and cultured for 24 h in the absence of thiamine. Cells were either untreated (basal) or treated with 500 mM NaCl and analyzed as in Figure 1D.

(Figure 3B, Δ*pmk1*). Moreover, when constitutively active MAPKK Pek1^{DD} was overexpressed in the wild-type cells, a significantly higher level of 3*x*CRE$_{ECM33}$::luc (R2.2) reporter response was observed even without any stimulation (Figure 3C, wt-Pek1^{DD} OP), and addition of NaCl to the medium further stimulated the response (Figure 3C, wt-Pek1^{DD} OP, +500 mM NaCl). This induction by Pek1^{DD} and the addition of NaCl was almost abolished in Δ*pmk1* cells (Figure 3C, Δ*pmk1*), indicating the Pmk1-dependent response of the 3*x*CRE$_{ECM33}$::luc (R2.2) reporter. It should be noted that the relative light units in Δ*pmk1* cells were ~20% of that of the wild-type cells and were relatively higher than those of the Δ*atf1* cells and Δ*sty1* cells. Thus, 3*x*CRE$_{ECM33}$::luc (R2.2) indicates both Sty1 and Pmk1 activation. The biphasic activation of the signal upon NaCl stimulation may reflect the intracellular Ca^{2+} concentration, i.e., the first sudden increase reflects the Ca^{2+} influx from the plasma membrane-localized Ca^{2+} channels, and the second increase indicates a mechanism similar to that of Ca^{2+}-induced Ca^{2+} release from the intracellular Ca^{2+} store.

To determine the cross-talk between Pmk1 and Sty1/Spc1 MAPK cascade in the regulation of Ecm33 transcription, we examined whether Pek1^{DD} overexpression can overcome the Δ*sty1* defect in the transcription from 3*x*CRE$_{ECM33}$. Pek1^{DD} overexpression failed to increase the transcription level of ECM33 from 3*x*CRE even after NaCl stimulation (Figure 3C, Δ*sty1*). This might be because of instability of the Atf1 protein in the absence of Sty1. Atf1 is a target for the ubiquitin-proteasome system (Lawrence *et al.*, 2009), and Sty1 phosphorylation of Atf1 is required for modulating Atf1 stability and is vital for a robust response to certain stresses (Lawrence *et al.*, 2007). Therefore, in the absence of the Sty1 protein, the Atf1 protein may be easily degraded and may fail to respond to Pmk1 activation by Pek1^{DD} overexpression.

Real-Time Monitoring of Mbx1 Activity in Living Cells

We next created the reporter construct 6*x*RLM$_{ECM33}$ fused to R2.2 destabilized luciferase [6*x*RLM$_{ECM33}$::luc (R2.2)]. As shown in Figure 4A, wild-type cells harboring the multicopy

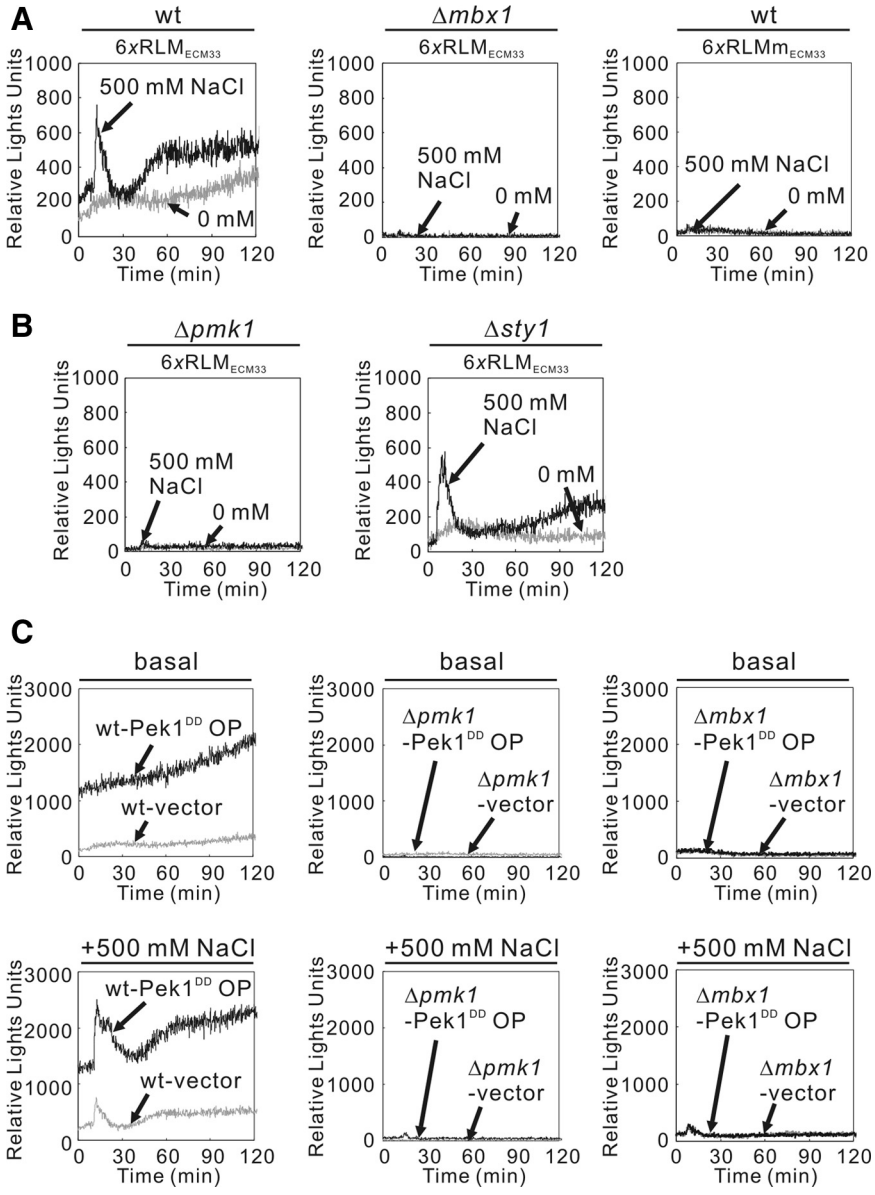

Figure 4. Real-time monitoring of Mbx1 activity in living cells. (A) Wild-type cells or Δ*mbx1* cells harboring the multicopy plasmid [6*x*RLM$_{ECM33}$::luc(R2.2) reporter vector] or the mutant version of the reporter vector [6*x*RLMm$_{ECM33}$::luc(R2.2)) were incubated with D-luciferin and treated with 500 mM NaCl. Using a luminometer, light emission levels expressed as relative light units were measured per min for 2 h. The data shown are representative of multiple experiments. (B) Live-cell monitoring of Mbx1 activity in Δ*pmk1* cells and Δ*sty1* cells. The cells as indicated were transformed with the multicopy plasmid [6*x*RLM$_{ECM33}$::luc(R2.2) reporter vector] and analyzed as described in A. (C) Overexpression of constitutively active Pek1 MAP kinase kinase stimulates Mbx1 activity. Wild-type, Δ*pmk1,* or Δ*mbx1* cells harboring the multicopy plasmid [6*x*RLM$_{ECM33}$::luc(R2.2) reporter vector] were transformed with either pREP2-Pek1^{DD} (Pek1^{DD} OP) or the control vector (vector) and cultured for 24 h in the absence of thiamine. Cells were either untreated (basal) or treated with 500 mM NaCl and analyzed as in Figure 1D.

6*x*RLM$_{ECM33}$::luc (R2.2) reporter were stimulated by the addition of 500 mM NaCl. Elevated extracellular NaCl also caused a rapid increase in the 6*x*RLM$_{ECM33}$::luc (R2.2) reporter response within 3 min, followed by a rapid decrease to reach its lowest value at around 30 min, then again showed a second increase, and finally approached a constant level (Figure 4A, wt). In contrast, the Δ*mbx1* cells harboring the same reporter showed minimal responses to the same stimuli, indicating that multicopy 6*x*RLM$_{ECM33}$::luc (R2.2) reporter could reflect the Mbx1 activity (Figure 4A, Δ*mbx1*). Disruption of *mbx2*$^{+}$ did not affect the promoter response (data not shown). Moreover, mutation at a consensus RLM site dramatically reduced the 6*x*RLM$_{ECM33}$::luc (R2.2) promoter activity with or without the stimuli (Figure 4A, wt, 6*x*RLMm$_{ECM33}$).

Notably, disruption of the *pmk1*$^{+}$ gene reduced the basal promoter activity and almost abolished the induction of the reporter by NaCl addition (Figure 4B, Δ*pmk1*). Sty1 deletion did not significantly affect the rapid response of the 6*x*RLM$_{ECM33}$::luc (R2.2) reporter, whereas the second increase in the reporter response to NaCl stimulation in Δ*sty1* cells was distinct from that in the wild-type cells (Figure 4B, Δ*sty1*). Thus, the rapid phase of the 6*x*RLM$_{ECM33}$::luc (R2.2) is a faithful reporter of Pmk1 pathway activation; Sty1 may also be involved in some aspects of the Mbx1 regulation.

Moreover, the overexpression of the constitutively active Pek1^{DD} induced reporter expression in wild-type cells even in the absence of stimulation (Figure 4C, wt-Pek1^{DD} OP, basal), and addition of NaCl to the medium further increased this response (Figure 4C, wt-Pek1^{DD} OP, +500 mM NaCl). This induction by Pek1^{DD} and its enhancement with the addition of NaCl were almost completely abolished in Δ*pmk1* cells, thereby indicating a Pmk1-dependent response of the 6*x*RLM$_{ECM33}$::luc (R2.2) reporter (Figure 4C, Δ*pmk1*). Moreover, the induction by Pek1^{DD} and its enhancement with the addition of NaCl were also abolished in Δ*mbx1* cells (Figure 4C, Δ*mbx1*). Thus, the Pek1^{DD}-induced transcription from 6*x*RLM $_{ECM33}$ observed in wild-type cells depends on the Mbx1 transcription factor.

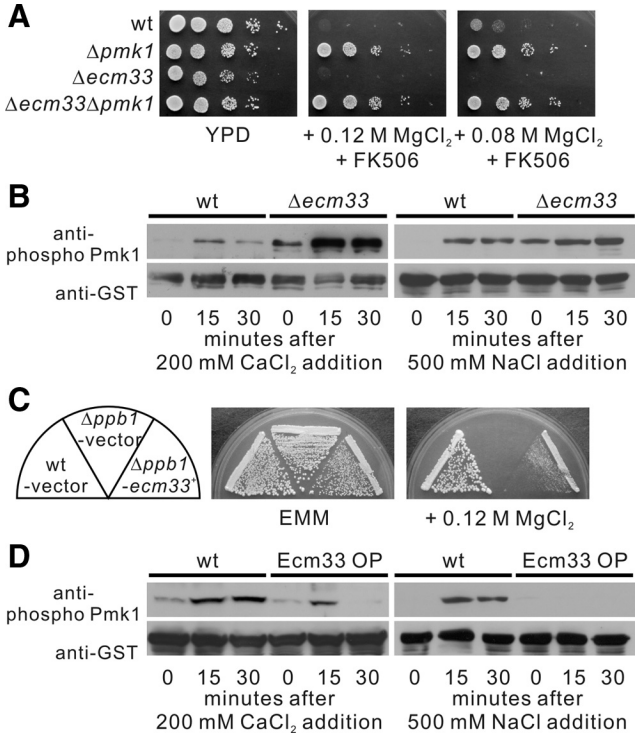

Figure 5. Ecm33 is involved in Pmk1 MAPK-mediated cell integrity signaling. (A) The *ecm33*$^+$ gene knockout displayed a *vic*-negative phenotype. The cells as indicated were spotted onto the plates and then incubated for 4 d at 27°C. (B) Knockout of the *ecm33*$^+$ gene stimulated the phosphorylation of Pmk1 MAPK. Wild-type or Δ*ecm33* cells harboring pREP41-GST-Pmk1 were grown to midlog phase in EMM and then incubated in EMM containing 200 mM $CaCl_2$, or 500 mM NaCl for the indicated time points; cells were collected and lysed at each time point. Immunoblotting using anti-phospho Pmk1 and anti-glutathione *S*-transferase (GST) antibodies showed that Pmk1 is hyperphosphorylated in the Δ*ecm33* cells. (C) Overexpression of *ecm33*$^+$ suppressed the Cl^- hypersensitivity of calcineurin deletion cells (Δ*ppb1*). Calcineurin-deleted cells containing either the multicopy plasmid carrying *ecm33*$^+$ or the control vector, or the wild-type cells carrying the control vector were grown in EMM or EMM containing 0.12 M $MgCl_2$. (D) Overexpression of *ecm33*$^+$ suppressed the phosphorylation of Pmk1. Wild-type cells transformed with pREP41-GST-Pmk1, containing either the control vector or the multicopy *ecm33*$^+$ gene, were grown to midlog phase in EMM and analyzed as in B.

Role of Ecm33 in Pmk1 Signaling

We previously demonstrated that mutations in the components of the Pmk1 pathway result in the *vic* phenotype (Ma *et al.*, 2006). These components include Pmk1 MAPK, Pek1 MAPKK, Mkh1 MAPKKK, Pck2 protein kinase C, and Rho2. We further examined the functional relationship between Ecm33 and Pmk1 signaling by analyzing whether the disruption of the *ecm33*$^+$ gene affected the chloride ion hypersensitivity induced by the inhibition of the protein phosphatase calcineurin by using the immunosuppressant FK506, a specific inhibitor of calcineurin (Sugiura *et al.*, 1998). The results showed that Δ*ecm33* cells, like wild-type cells, failed to grow in the presence of the immunosuppressant FK506 and 0.12 M $MgCl_2$, whereas Δ*pmk1* cells grew well under these conditions (Figure 5A, +0.12 M $MgCl_2$ +FK506). Moreover, Δ*ecm33* cells failed to grow in the presence of the immunosuppressant FK506 and 0.08 M $MgCl_2$, wherein wild-type cells grew slowly (Figure 5A, +0.08 M $MgCl_2$ +FK506). Thus, Ecm33 deletion exacerbated the chloride ion hypersensitivity induced by calcineurin inhibition. In our previous study, we showed that the hyperactivation of Pmk1 MAPK by the overexpression of the constitutively active Pek1^{DD} exacerbated the chloride ion hypersensitivity of calcineurin deletion (Sugiura *et al.*, 1999). This suggested that Ecm33 deletion, like Pek1^{DD}, induced hyperactivation of Pmk1 signaling. To investigate this possibility, we examined the level of Pmk1 phosphorylation in Δ*ecm33* cells using anti-phospho Pmk1 antibodies that recognize only phosphorylated and hence activated Pmk1 (Sugiura *et al.*, 1999). The results revealed that Δ*ecm33* cells showed increased Pmk1 phosphorylation level compared with that of the wild-type cells under normal conditions(Figure 5B, 0 min). Moreover, upon treatment with $CaCl_2$, the phosphorylation of Pmk1 was greatly induced in Δ*ecm33* cells than in wild-type cells (Figure 5B, left panel). Further, the addition of 500 mM NaCl induced a higher-than-normal level of Pmk1 phosphorylation in Δ*ecm33* cells (Figure 5B, right panel). Consistently, the *vic*-negative phenotype associated with Δ*ecm33* cells was rescued by Pmk1 deletion, because the Δ*ecm33*Δ*pmk1* double mutant cells grew well in the presence of the immunosuppressant FK506 and 0.12 M $MgCl_2$ as did Δ*pmk1* cells (Figure 5A, Δ*ecm33*Δ*pmk1*). In addition, disruption of the *rho2*$^+$ gene, an upstream activator of the Pmk1 pathway, also rescued the *vic*-negative phenotype of Δ*ecm33* cells (data not shown). Thus, loss of Ecm33 function induced hyperactivation of the Rho2/Pmk1 cell integrity pathway.

We next examined the effect of the overexpression of Ecm33 on the chloride ion hypersensitivity of calcineurin deletion (Δ*ppb1*). Our previous data showed that overexpression of the dual-specificity phosphatase Pmp1 or the type 2C phosphatases Ptc1 or Ptc3 suppressed the chloride ion hypersensitivity of Δ*ppb1* cells by inhibiting Pmk1 activation (Sugiura *et al.*, 1998; Takada *et al.*, 2007). If Ecm33 were considered to play a role in the negative regulation of Pmk1 signaling, it would be expected that Ecm33 overexpression would also suppress Δ*ppb1* cells. As expected, Δ*ppb1* cells overexpressing the *ecm33*$^+$ gene could grow in the presence of 0.12 M $MgCl_2$, whereas those bearing the control vector alone failed to grow (Figure 5C). Moreover, the overexpression of the *ecm33*$^+$ gene almost abolished the stimulation of Pmk1 phosphorylation both before and after $CaCl_2$ treatment (Figure 5D, Ecm33 OP, left panel). The inhibitory effect of Ecm33 overproduction on Pmk1 phosphorylation was also observed when cells were treated with 500 mM NaCl (Figure 5D, right panel).

Knockout of the pmk1$^+$ *Gene Rescued Phenotypes of* Δ*ecm33 Cells*

Another striking feature of Δ*ecm33* cells is their hypersensitivity to $CaCl_2$. As shown in Figure 6A, Δ*ecm33* cells grew poorly in the media supplemented with 150 mM $CaCl_2$, whereas wild-type cells grew normally. In contrast, Δ*ecm33* cells grew well in the media supplemented with 150 mM $MgCl_2$ or 300 mM NaCl, suggesting that Ca^{2+} homeostasis is altered in Δ*ecm33* cells (Figure 6A). Moreover, the Ca^{2+}-hypersensitive phenotype observed in Δ*ecm33* cells was rescued by Pmk1 deletion (Figure 6A, Δ*ecm33*Δ*pmk1*), suggesting that this phenotype somehow results from Pmk1 hyperactivation in Δ*ecm33* cells. In addition, morphologically, the Δ*ecm33* cells were abnormally enlarged and swollen compared with the wild-type cells (Figure 6B, Δ*ecm33*). Notably, simultaneous deletion of Pmk1 almost rescued the morphological abnormality observed in Δ*ecm33* cells (Figure 6B, Δ*ecm33*Δ*pmk1*). Interestingly, the above finding that Pmk1 deletion rescued Δ*ecm33* phenotypes clearly contrasts the re-

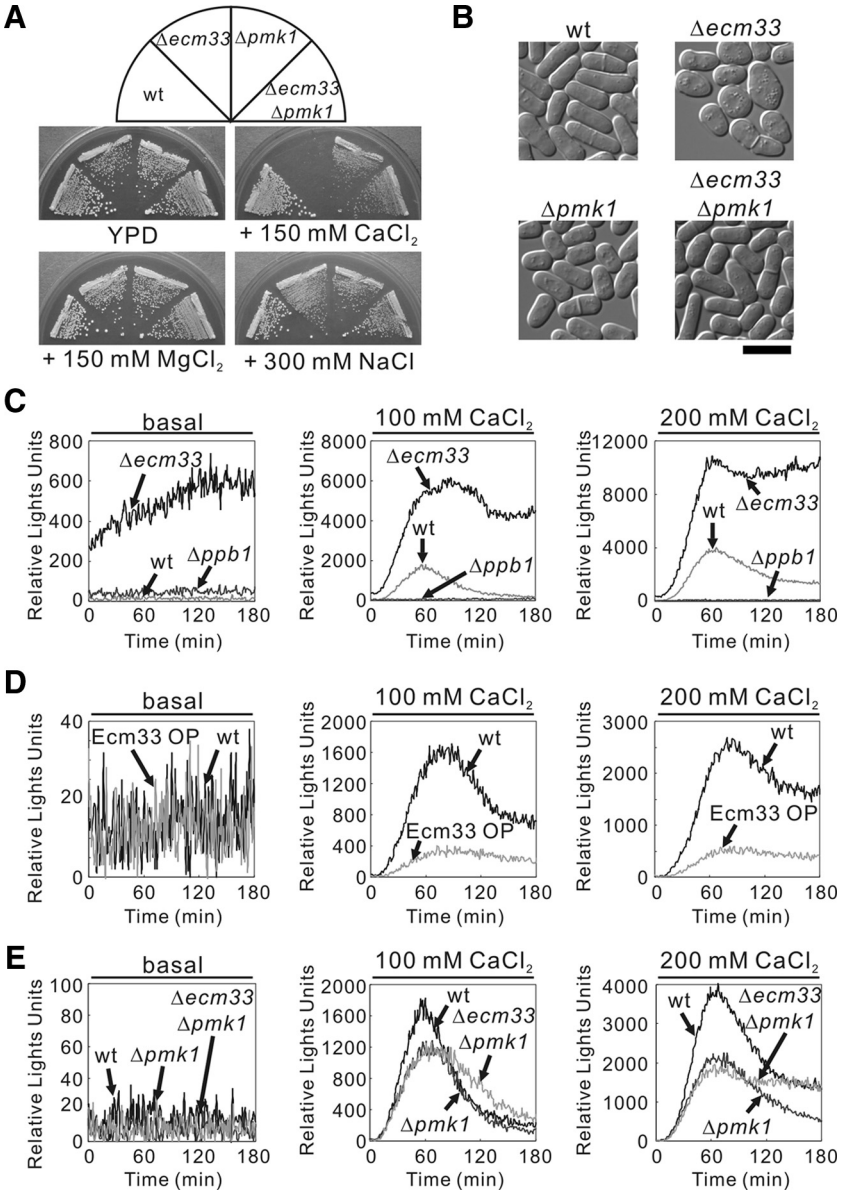

Figure 6. Altered Ca^{2+} homeostasis in Δ*ecm33* cells. (A) Δ*ecm33* cells exhibited Ca^{2+} hypersensitivity. Wild-type cells, Δ*ecm33*, Δ*pmk1*, or Δ*ecm33*Δ*pmk1* cells were streaked onto the plates as indicated and then incubated for 4 d at 27°C. (B) Δ*ecm33* cells exhibited abnormal morphology. Morphology of the wild-type cells, Δ*ecm33*, Δ*pmk1*, or Δ*ecm33*Δ*pmk1* cells incubated in YPD liquid medium. Scale bar, 10 μm. (C) Δ*ecm33* cells displayed an enhanced calcineurin activity. Wild-type cells, Δ*ecm33*, or Δ*ppb1* cells harboring the multicopy plasmid [3*x*CDRE::luc(R2.2)] reporter vector were incubated with D-luciferin and treated with various concentrations of $CaCl_2$ and then were analyzed as in Figure 1D. (D) Wild-type cells harboring the multicopy plasmid [3*x*CDRE::luc(R2.2)] reporter vector were transformed with either the control vector (vector) or the *ecm33*$^+$ gene (Ecm33 OP) and then analyzed as in Figure 6(C). (E) Pmk1 deletion suppressed the enhanced calcineurin activity in Δ*ecm33* cells. Wild-type, Δ*pmk1*, or Δ*ecm33*Δ*pmk1* cells harboring the multicopy plasmid [3*x*CDRE::luc(R2.2)] reporter vector were analyzed for calcineurin activity as in Figure 6C.

port in budding yeast where simultaneous deletion of *ECM33* and *SLT2* results in synthetic lethality (Pardo *et al.*, 2004).

Altered Calcium Homeostasis in Δecm33 Cells

To further characterize the Ca^{2+}-related phenotypes associated with Δ*ecm33* cells, we used the 3*x*CDRE::luc(R2.2) reporter system that was developed to monitor the real-time activity of the Ca^{2+}/calcineurin signaling pathway (Deng *et al.*, 2006). We assumed that if Ca^{2+} homeostasis is compromised in Δ*ecm33* cells, the CDRE reporter response would be altered from that of the wild-type cells. As shown in Figure 6C, the Δ*ecm33* cells showed an enhanced 3*x*CDRE::luc(R2.2) reporter response in the presence of various concentrations of extracellular $CaCl_2$ (0–200 mM), compared with that of the wild-type cells. Notably, compared with the wild-type cells, Δ*ecm33* cells showed a continuous increase in the 3*x*CDRE::luc(R2.2) response (Figure 6C, 100 mM $CaCl_2$, 200 mM $CaCl_2$). The enhanced calcineurin activity as evidenced by the CDRE response and Ca^{2+} hypersensitivity of Δ*ecm33* cells is reminiscent of that observed in Δ*pmc1* cells, which lack the vacuolar Ca^{2+}-ATPase (Deng *et al.*, 2006). On the other hand, the overproduction of Ecm33 (Ecm33 OP) lowered the CDRE response even in the presence of 200 mM $CaCl_2$ (Figure 6D, 100 mM $CaCl_2$, 200 mM $CaCl_2$).

We further examined the effect of Pmk1 deletion on the CDRE reporter response. In the presence of 100 mM $CaCl_2$, the Δ*pmk1* cells exhibited a slightly lower peak response of the CDRE reporter than the wild-type cells. In the presence of 200 mM $CaCl_2$, the peak response of the Δ*pmk1* cells was approximately half that of the wild-type cells (Figure 6E, Δ*pmk1*). Importantly, the peak responses of the CDRE reporter in the Δ*ecm33*Δ*pmk1* cells were almost similar to those in the Δ*pmk1* cells suggesting that the increased Ca^{2+}/calcineurin signaling observed in the Δ*ecm33* mutant is dependent on Pmk1. However, the calcineurin activity remains higher in the Δ*ecm33*Δ*pmk1* cells than in the Δ*pmk1* cells, after the peak response to $CaCl_2$stimulation has been attainted (Figure 6E, 200 mM $CaCl_2$).

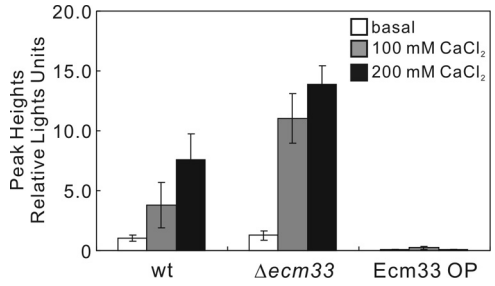

Figure 7. Ecm33 regulates Ca^{2+} influx. The peak response of intracellular Ca^{2+} monitoring after the addition of $CaCl_2$. Wild-type, Δ*ecm33*, and cells overproducing Ecm33 (Ecm33 OP) were transformed with pREP1-AEQ, and their intracellular Ca^{2+} levels were monitored during the first 10 min. Cells were either untreated or treated with 100 mM $CaCl_2$ or 200 mM $CaCl_2$. The aequorin assay was performed as described in *Materials and Methods*. The data were averaged from peak heights of three independent experiments, and each sample was done in duplicate. Error bars, SD.

To provide additional information regarding the defective Ca^{2+} homeostasis in Δ*ecm33* cells, we monitored intracellular Ca^{2+} levels in wild-type and Δ*ecm33* cells. The Δ*ecm33* cells displayed a higher Ca^{2+} concentration than that observed in the wild-type cells in terms of the level of peak response (Figure 7). In contrast, intracellular Ca^{2+} levels in cells overexpressing the *ecm33*$^+$ gene were significantly lower than those in the cells bearing the control vector alone (Figure 7, Ecm33 OP). Taken together, the results suggest that Ecm33 might exert its effect on Pmk1 signaling by affecting Ca^{2+} homeostasis in fission yeast.

DISCUSSION

In the present study, the identification of Ecm33 as a novel component of the Pmk1 MAPK cell integrity signaling has led to the discovery that two transcription factors, namely, Atf1 and Mbx1, are involved in the Pmk1-dependent expression of Ecm33. We also developed a reporter system to monitor the real-time activity of these transcription factors and hence the activation of the Pmk1 pathway.

Here, we show that Ecm33 is involved in the cell integrity signaling. First, mutants lacking *ecm33*$^+$ displayed hypersensitivity to two typical cell wall–damaging agents, calcofluor white and β-glucanase. Second, Δ*ecm33* cells exhibited the *vic*-negative phenotype and hyperphosphorylation of the Pmk1 MAPK, which is a strong indication of the negative regulation of the Pmk1 signaling (Ma *et al.*, 2006). Third, Ecm33 overproduction suppressed calcineurin deletion and inhibited Pmk1 MAPK phosphorylation upon treatment with $CaCl_2$ and NaCl. Fourth, the mRNA levels of *ecm33*$^+$ were Pmk1/Atf1– as well as Pmk1-Mbx1–dependent. Thus, Ecm33 is a novel component of the Pmk1 MAPK pathway.

In budding yeast, signaling via Mpk1-Rlm1 regulates the expression of several genes implicated in cell wall biogenesis, including PST1 (Jung and Levin, 1999; Jung *et al.*, 2002). Unexpectedly, the deletion mutants of Mbx2, an Rlm1 homologue in fission yeast, displayed only modest sensitivity to cell wall–damaging agents, such as calcofluor (Figure 2E), suggesting that unlike budding yeast, the Rlm1 homolog only plays a minor role in cell wall integrity in fission yeast. Here, we identified Ecm33, a cell surface GPI-anchor protein homologous to PST1, as a target of Pmk1 and Atf1. Moreover, Mbx1, but not Mbx2, was found to be involved in the regulation of Ecm33 expression (Figure 2D). Mbx1 has been shown to be involved in gene expression in the M-G1 phase as a component of PBF (Pombe cell cycle box binding factor) transcriptional complex (Buck *et al.*, 2004). Although Mbx1 genetically and functionally interacts with two forkhead transcription factors Fkh2 and Sep1 together with Plo1, the direct target of Mbx1 and its physiological role have not yet been elucidated; this is because the deletion of *mbx1*$^+$ has little effect on M–G1 transcription (Papadopoulou *et al.*, 2008). In this study, we showed that Mbx1 is involved in cell integrity in fission yeast via the regulation of Ecm33 in a Pmk1-dependent manner. Recently, Papadopoulou *et al.* (2008) reported that the Polo kinase Plo1, a key regulator of cell cycle, binds and phosphorylates Mbx1. It would be intriguing to speculate that Plo1 and Pmk1 kinases coordinately regulate cell cycle and/or cell integrity signaling via the phospho-regulation of Mbx1 activity.

Another important finding of this study is the role of Ecm33 in the MAPK cell integrity signaling. The finding that Ecm33 deletion and overproduction affect Ca^{2+}/calcineurin signaling and Ca^{2+} homeostasis suggested the possibility that some Ca^{2+}-mobilizing mechanism(s) might be involved in the Ecm33-mediated suppression of Pmk1 signaling. Carnero *et al.* (2000) reported that *ehs1*$^+$*/yam8*$^+$, encoding a homologue of the budding yeast Mid1, is involved in Ca^{2+} accumulation and cell wall integrity. Interestingly, high extracellular levels of Ca^{2+} as well as *pck2*$^+$ overexpression suppressed all the phenotypes of *ehs1/yam8* mutants, suggesting that the cell integrity defects of *ehs1/yam8* mutant

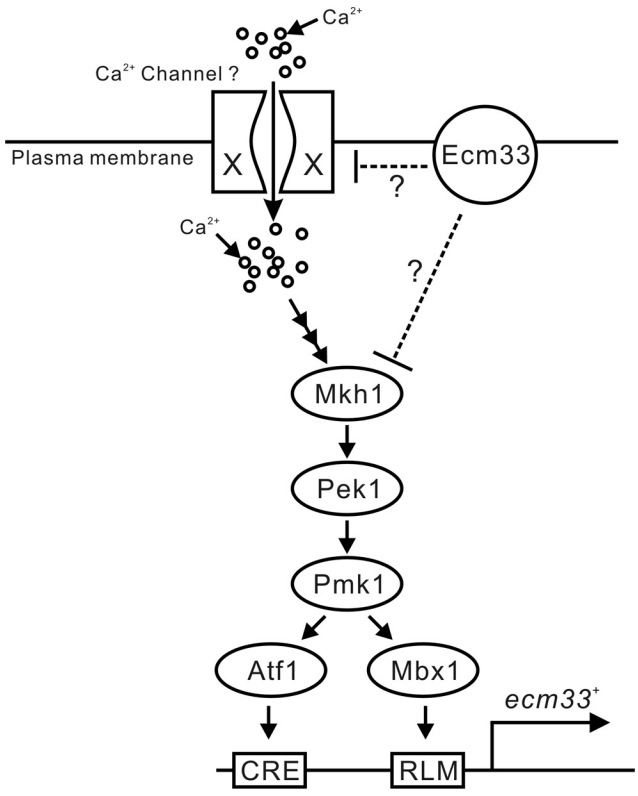

Figure 8. A model for the dual regulation of *ecm33*$^+$ gene expression and its putative involvement in the negative feedback regulation of the Pmk1 MAPK signaling pathway. Regulatory elements in the promoter are schematically represented. Dotted lines denote hitherto uncharacterized processes. Ecm33 may exert its effect on Ca^{2+}/calcineurin signaling largely via Pmk1 pathway and partly via other Ca^{2+}-influx machineries.

result from inadequate calcium levels in the cell (Carnero *et al.*, 2000). Similarly, our recent study showed that Pmk1 is required for the stimulation of calcineurin via Yam8/Cch1-mediated Ca^{2+} influx and that knockout of *pck2*$^{+}$ gene markedly diminished the Yam8/Cch1-dependent stimulation of calcineurin activity, suggesting that Pck2 acts upstream of Pmk1 in this signaling pathway (Deng *et al.*, 2006). Thus, exogenous Ca^{2+} activates the Pck2/Pmk1 signaling, which in turn leads to Yam8/Cch1-mediated Ca^{2+} influx. The hyperactivation of Pck2/Pmk1 signaling induces lethality associated with strong Ca^{2+} accumulation (Carnero *et al.*, 2000; Deng *et al.*, 2006). One way to reverse this effect is by the dephosphorylation and inactivation of Pmk1 via the overexpression of Pmp1 or PP2C phosphatases as evidenced in our previous studies (Sugiura *et al.*, 1998; Takada *et al.*, 2007). Alternatively, inactivation of the Ca^{2+}-influx machinery, such as Yam8/Cch1 complex, and maintenance of the normal Ca^{2+} homeostasis within the cell would also rescue cells from the lethal effect.

The molecular mechanism underlying Ecm33-mediated modulation of Pmk1 signaling is currently unknown. Given the plasma membrane localization of Ecm33, we hypothesize that Ecm33, a GPI-anchored protein, like the sensor protein Wsc1 in budding yeast (Philip and Levin, 2001), might interact with some component(s) of the plasma membrane localizing MAPK signaling molecules and/or the components of Ca^{2+}-influx machinery to inhibit protein function (Figure 8). Our results showed that Ecm33 deletion and overproduction affects Pmk1 phosphorylation upon treatment with $CaCl_2$ and NaCl, two independent stimuli that activate Pmk1 (Figure 5, B and D). Moreover, Pmk1 deletion markedly suppressed the increased Ca^{2+}/calcineurin signaling observed in Δ*ecm33* cells (Figure 6E). These results favor the possibility that Ecm33 impinges on the Pmk1 MAPK cascade via a Ca^{2+}-independent mechanism and that Pmk1 then regulates Ca^{2+} influx. However, Δ*ecm33*Δ*pmk1* cells exhibited a higher CDRE reporter activity than the Δ*pmk1* cells after the peak response (Figure 6E), and Ecm33 overproduction resulted in a lower CDRE response than that in Δ*pmk1* cells upon in the $CaCl_2$ treatment (Figure 6D). Thus, it does not exclude the possibility that Ecm33 may exert its effect on Ca^{2+}/calcineurin signaling largely via Pmk1 pathway and partly via other Ca^{2+}-influx machineries (Figure 8). Further studies will be required to clarify the precise role of Ecm33 and its involvement in the MAPK signaling.

In conclusion, to our knowledge, this article provides the first evidence for the involvement of a GPI-anchored cell surface protein in the negative regulation of cell wall integrity Pmk1 MAPK signaling. Furthermore, we also discovered a novel functional link between Ecm33 and cellular Ca^{2+} signaling. Given the high similarity between the MAPK pathways of fission yeast and the mammals, this study may provide the basis of understanding the regulatory mechanisms underlying MAPK signaling in higher eukaryotes.

ACKNOWLEDGMENTS

We thank Drs. M. Yanagida, and T. Toda and Yeast Resource Centre (YGRC/NBRP; http://yeast.lab.nig.ac.jp/nig) for providing strains and plasmids; Kazue Masuko for able technical assistance; and Susie O. Sio and Yukiko Fujimoto for critical reading of the manuscript. We are grateful to the members of the Laboratory of Molecular Pharmacogenomics for their support. This work was supported by Grant-in-Aid for Scientific Research on Innovative Areas and research grants from the Ministry of Education, Culture, Sports, Science, and Technology of Japan (R.S.). This work was also financially supported by the Antiaging Center Project for Private Universities from Ministry of Education, Culture, Sports, Science, and Technology, 2008–2012. H.T. is a Research Fellow of the Japan Society for the Promotion of Science.

REFERENCES

Agarwal, A. K., Rogers, P. D., Baerson, S. R., Jacob, M. R., Barker, K. S., Cleary, J. D., Walker, L. A., Nagle, D. G., and Clark, A. M. (2003). Genome-wide expression profiling of the response to polyene, pyrimidine, azole, and echinocandin antifungal agents in *Saccharomyces cerevisiae.* J. Biol. Chem. *278*, 34998–35015.

Bahler, J., Wu, J. Q., Longtine, M. S., Shah, N. G., McKenzie, A., III, Steever, A. B., Wach, A., Philippsen, P., and Pringle, J. R. (1998). Heterologous modules for efficient and versatile PCR-based gene targeting in *Schizosaccharomyces pombe.* Yeast *14*, 943–951.

Buck, V., Ng, S. S., Ruiz-Garcia, A. B., Papadopoulou, K., Bhatti, S., Samuel, J. M., Anderson, M., Millar, J. B., and McInerny, C. J. (2004). Fkh2p and Sep1p regulate mitotic gene transcription in fission yeast. J. Cell Sci. *117*, 5623–5632.

Carnero, E., Ribas, J. C., Garcia, B., Duran, A., and Sanchez, Y. (2000). *Schizosaccharomyces pombe* ehs1p is involved in maintaining cell wall integrity and in calcium uptake. Mol. Gen. Genet. *264*, 173–183.

De Groot, P. W., Hellingwerf, K. J., and Klis, F. M. (2003). Genome-wide identification of fungal GPI proteins. Yeast *20*, 781–796.

Deng, L., Sugiura, R., Takeuchi, M., Suzuki, M., Ebina, H., Takami, T., Koike, A., Iba, S., and Kuno, T. (2006). Real-time monitoring of calcineurin activity in living cells: evidence for two distinct Ca^{2+}-dependent pathways in fission yeast. Mol. Biol. Cell *17*, 4790–4800.

Edmunds, J. W., and Mahadevan, L. C. (2004). MAP kinases as structural adaptors and enzymatic activators in transcription complexes. J. Cell Sci. *117*, 3715–3723.

Gustin, M. C., Albertyn, J., Alexander, M., and Davenport, K. (1998). MAP kinase pathways in the yeast *Saccharomyces cerevisiae.* Microbiol. Mol. Biol. Rev. *62*, 1264–1300.

Herskowitz, I. (1995). MAP kinase pathways in yeast: for mating and more. Cell *80*, 187–197.

Hirayama, S., Sugiura, R., Lu, Y., Maeda, T., Kawagishi, K., Yokoyama, M., Tohda, H., Hama, Y. G., Shuntoh, H., and Kuno, T. (2003). Zinc finger protein Prz1 regulates Ca^{2+} but not Cl^{-} homeostasis in fission yeast: identification of distinct branches of calcineurin signaling pathway in fission yeast. J. Biol. Chem. *278*, 18078–18084.

Jung, U. S., and Levin, D. E. (1999). Genome-wide analysis of gene expression regulated by the yeast cell wall integrity signalling pathway. Mol. Microbiol. *34*, 1049–1057.

Jung, U. S., Sobering, A. K., Romeo, M. J., and Levin, D. E. (2002). Regulation of the yeast Rlm1 transcription factor by the Mpk1 cell wall integrity MAP kinase. Mol. Microbiol. *46*, 781–789.

Kohrer, K., and Domdey, H. (1991). Preparation of high molecular weight RNA. Methods Enzymol. *194*, 398–405.

Lawrence, C. L., Jones, N., and Wilkinson, C. R. (2009). Stress-induced phosphorylation of *S. pombe* Atf1 abrogates its interaction with F box protein Fbh1. Curr. Biol. *19*, 1907–1911.

Lawrence, C. L., Maekawa, H., Worthington, J. L., Reiter, W., Wilkinson, C. R., and Jones, N. (2007). Regulation of *Schizosaccharomyces pombe* Atf1 protein levels by Sty1-mediated phosphorylation and heterodimerization with Pcr1. J. Biol. Chem. *282*, 5160–5170.

Leskinen, P., Virta, M., and Karp, M. (2003). One-step measurement of firefly luciferase activity in yeast. Yeast *20*, 1109–1113.

Levin, D. E., and Errede, B. (1995). The proliferation of MAP kinase signaling pathways in yeast. Curr. Opin. Cell Biol. *7*, 197–202.

Ma, Y., Kuno, T., Kita, A., Asayama, Y., and Sugiura, R. (2006). Rho2 is a target of the farnesyltransferase Cpp1 and acts upstream of Pmk1 mitogen-activated protein kinase signaling in fission yeast. Mol. Biol. Cell *17*, 5028–5037.

Madrid, M., Soto, T., Khong, H. K., Franco, A., Vicente, J., Perez, P., Gacto, M., and Cansado, J. (2006). Stress-induced response, localization, and regulation of the Pmk1 cell integrity pathway in *Schizosaccharomyces pombe.* J. Biol. Chem. *281*, 2033–2043.

Marshall, C. J. (1994). MAP kinase kinase kinase, MAP kinase kinase and MAP kinase. Curr. Opin. Genet. Dev. *4*, 82–89.

Moreno, S., Klar, A., and Nurse, P. (1991). Molecular genetic analysis of fission yeast *Schizosaccharomyces pombe.* Methods Enzymol. *194*, 795–823.

Nishida, E., and Gotoh, Y. (1993). The MAP kinase cascade is essential for diverse signal transduction pathways. Trends Biochem. Sci. *18*, 128–131.

Ohno, Y., Yagi, H., Nakamura, M., Masuko, K., Hashimoto, Y., and Masuko, T. (2008). Cell-death-inducing monoclonal antibodies raised against DT40 tumor cells: identification of chicken transferrin receptor as a novel cell-death receptor. Cancer Sci. *99*, 894–900.

Pascual-Ahuir, A., Serrano, R., and Proft, M. (2001). The Sko1P repressor and Gcn4P activator antagonistically modulate strees-regulated transcription in *Saccharomyces cerevisiae*. Mol. Cell Biol. *21*, 16–25.

Papadopoulou, K., Ng, S. S., Ohkura, H., Geymonat, M., Sedgwick, S. G., and McInerny, C. J. (2008). Regulation of gene expression during M-G1-phase in fission yeast through Plo1p and forkhead transcription factors. J. Cell Sci. *121*, 38–47.

Pardo, M., Monteoliva, L., Vazquez, P., Martinez, R., Molero, G., Nombela, C., and Gil, C. (2004). PST1 and ECM33 encode two yeast cell surface GPI proteins important for cell wall integrity. Microbiology *150*, 4157–4170.

Philip, B., and Levin, D. E. (2001). Wsc1 and Mid2 are cell surface sensors for cell wall integrity signaling that act through Rom2, a guanine nucleotide exchange factor for Rho1. Mol. Cell. Biol. *21*, 271–280.

Pouyssegur, J. (2000). Signal transduction. An arresting start for MAPK. Science *290*, 1515–1518.

Rothstein, R. J. (1983). One-step gene disruption in yeast. Methods Enzymol. *101*, 202–211.

Satoh, R., *et al*. (2009). Role of the RNA-binding protein Nrd1 and Pmk1 mitogen-activated protein kinase in the regulation of myosin mRNA stability in fission yeast. Mol. Biol. Cell *20*, 2473–2485.

Sengar, A. S., Markley, N. A., Marini, N. J., and Young, D. (1997). Mkh1, a MEK kinase required for cell wall integrity and proper response to osmotic and temperature stress in *Schizosaccharomyces pombe*. Mol. Cell. Biol. *17*, 3508–3519.

Sio, S. O., Suehiro, T., Sugiura, R., Takeuchi, M., Mukai, H., and Kuno, T. (2005). The role of the regulatory subunit of fission yeast calcineurin for in vivo activity and its relevance to FK506 sensitivity. J. Biol. Chem. *280*, 12231–12238.

Sugiura, R., Kita, A., and Kuno, T. (2004). Upregulation of mRNA in MAPK signaling: transcriptional activation or mRNA stabilization? Cell Cycle *3*, 286–288.

Sugiura, R., Kita, A., Shimizu, Y., Shuntoh, H., Sio, S. O., and Kuno, T. (2003). Feedback regulation of MAPK signalling by an RNA-binding protein. Nature *424*, 961–965.

Sugiura, R., Sio, S. O., Shuntoh, H., and Kuno, T. (2002). Calcineurin phosphatase in signal transduction: lessons from fission yeast. Genes Cells *7*, 619–627.

Sugiura, R., Toda, T., Dhut, S., Shuntoh, H., and Kuno, T. (1999). The MAPK kinase Pek1 acts as a phosphorylation-dependent molecular switch. Nature *399*, 479–483.

Sugiura, R., Toda, T., Shuntoh, H., Yanagida, M., and Kuno, T. (1998). $pmp1^{+}$, a suppressor of calcineurin deficiency, encodes a novel MAP kinase phosphatase in fission yeast. EMBO J. *17*, 140–148.

Takada, H., *et al*. (2007). Atf1 is a target of the mitogen-activated protein kinase Pmk1 and regulates cell integrity in fission yeast. Mol. Biol. Cell *18*, 4794–4802.

Thai, M. V., Guruswamy, S., Cao, K. T., Pessin, J. E., and Olson, A. L. (1998). Myocyte enhancer factor 2 (MEF2)-binding site is required for GLUT4 gene expression transgenic mice. J. Biol. Chem. *273*, 14285–14292.

Toda, T., Dhut, S., Superti, F. G., Gotoh, Y., Nishida, E., Sugiura, R., and Kuno, T. (1996). The fission yeast $pmk1^{+}$ gene encodes a novel mitogen-activated protein kinase homolog which regulates cell integrity and functions coordinately with the protein kinase C pathway. Mol. Cell. Biol. *16*, 6752–6764.

Tougan, T., Chiba, Y., Kakihara, Y., Hirata, A., and Nojima, H. (2002). Meu10 is required for spore wall maturation in *Schizosaccharomyces pombe*. Genes Cells *7*, 217–231.

Wilkinson, M. G., Samuels, M., Takeda, T., Toone, W. M., Shieh, J. C., Toda, T., Millar, J. B., and Jones, N. (1996). The Atf1 transcription factor is a target for the Sty1 stress-activated MAP kinase pathway in fission yeast. Genes Dev. *10*, 2289–2301.

Zaitsevskaya-Carter, T., and Cooper, J. A. (1997). Spm1, a stress-activated MAP kinase that regulates morphogenesis in *S. pombe*. EMBO J. *16*, 1318–1331.